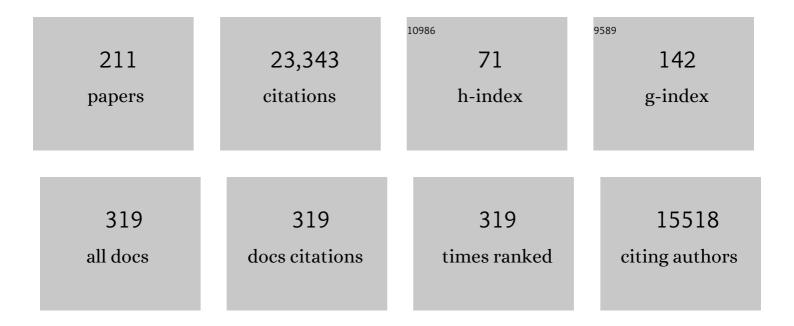
Colm Sweeney

List of Publications by Year in descending order

Source: https://exaly.com/author-pdf/4558151/publications.pdf Version: 2024-02-01



#	Article	IF	CITATIONS
1	The NASA Atmospheric Tomography (ATom) Mission: Imaging the Chemistry of the Global Atmosphere. Bulletin of the American Meteorological Society, 2022, 103, E761-E790.	3.3	39
2	Permafrost carbon emissions in a changing Arctic. Nature Reviews Earth & Environment, 2022, 3, 55-67.	29.7	124
3	Carbon Monoxide Emissions from the Washington, DC, and Baltimore Metropolitan Area: Recent Trend and COVID-19 Anomaly. Environmental Science & Technology, 2022, 56, 2172-2180.	10.0	7
4	H ₂ O ₂ and CH ₃ OOH (MHP) in the Remote Atmosphere: 1. Global Distribution and Regional Influences. Journal of Geophysical Research D: Atmospheres, 2022, 127, .	3.3	11
5	Continental-scale contributions to the global CFC-11 emission increase between 2012 and 2017. Atmospheric Chemistry and Physics, 2022, 22, 2891-2907.	4.9	2
6	Global nature run data with realistic high-resolution carbon weather for the year of the Paris Agreement. Scientific Data, 2022, 9, 160.	5.3	3
7	Global Carbon Budget 2021. Earth System Science Data, 2022, 14, 1917-2005.	9.9	663
8	Using atmospheric trace gas vertical profiles to evaluate model fluxes: a case study of Arctic-CAP observations and GEOS simulations for the ABoVE domain. Atmospheric Chemistry and Physics, 2022, 22, 6347-6364.	4.9	6
9	Satellite soil moisture data assimilation impacts on modeling weather variables and ozone in the southeastern US – Part 2: Sensitivity to dry-deposition parameterizations. Atmospheric Chemistry and Physics, 2022, 22, 7461-7487.	4.9	4
10	Technical note: A high-resolution inverse modelling technique for estimating surface CO ₂ fluxes based on the NIES-TM–FLEXPART coupled transport model and its adjoint. Atmospheric Chemistry and Physics, 2021, 21, 1245-1266.	4.9	23
11	Evaluation of single-footprint AIRS CH ₄ profile retrieval uncertainties using aircraft profile measurements. Atmospheric Measurement Techniques, 2021, 14, 335-354.	3.1	15
12	Carbon Monitoring System Flux Net Biosphere Exchange 2020 (CMS-Flux NBE 2020). Earth System Science Data, 2021, 13, 299-330.	9.9	40
13	Quantifying Nitrous Oxide Emissions in the U.S. Midwest: A Topâ€Down Study Using High Resolution Airborne Inâ€Situ Observations. Geophysical Research Letters, 2021, 48, e2020GL091266.	4.0	8
14	Retrieval of atmospheric CO ₂ vertical profiles from ground-based near-infrared spectra. Atmospheric Measurement Techniques, 2021, 14, 3087-3118.	3.1	14
15	Boreal forest fire CO and CH ₄ emission factors derived from tower observations in Alaska during the extreme fire season of 2015. Atmospheric Chemistry and Physics, 2021, 21, 8557-8574.	4.9	17
16	Impact of stratospheric air and surface emissions on tropospheric nitrous oxide during ATom. Atmospheric Chemistry and Physics, 2021, 21, 11113-11132.	4.9	5
17	Atmospheric Carbon and Transport – America (ACTâ€America) Data Sets: Description, Management, and Delivery. Earth and Space Science, 2021, 8, e2020EA001634.	2.6	15
18	COS-derived GPP relationships with temperature and light help explain high-latitude atmospheric CO ₂ seasonal cycle amplification. Proceedings of the National Academy of Sciences of the United States of America, 2021, 118, .	7.1	21

#	Article	IF	CITATIONS
19	Covariation of Airborne Biogenic Tracers (CO ₂ , COS, and CO) Supports Stronger Than Expected Growing Season Photosynthetic Uptake in the Southeastern US. Global Biogeochemical Cycles, 2021, 35, e2021GB006956.	4.9	7
20	Tropospheric Ageâ€ofâ€Air: Influence of SF ₆ Emissions on Recent Surface Trends and Model Biases. Journal of Geophysical Research D: Atmospheres, 2021, 126, e2021JD035451.	3.3	3
21	The Atmospheric Carbon and Transport (ACT)-America Mission. Bulletin of the American Meteorological Society, 2021, 102, E1714-E1734.	3.3	17
22	Relative flux measurements of biogenic and natural gas-derived methane for seven U.S. cities. Elementa, 2021, 9, .	3.2	7
23	Methane Growth Rate Estimation and Its Causes in Western Canada Using Satellite Observations. Journal of Geophysical Research D: Atmospheres, 2021, 126, e2020JD033948.	3.3	1
24	Seasonal Variability in Local Carbon Dioxide Biomass Burning Sources Over Central and Eastern US Using Airborne In Situ Enhancement Ratios. Journal of Geophysical Research D: Atmospheres, 2021, 126, e2020JD034525.	3.3	8
25	Strong Southern Ocean carbon uptake evident in airborne observations. Science, 2021, 374, 1275-1280.	12.6	44
26	Multispecies Assessment of Factors Influencing Regional CO ₂ and CH ₄ Enhancements During the Winter 2017 ACTâ€America Campaign. Journal of Geophysical Research D: Atmospheres, 2020, 125, e2019JD031339.	3.3	23
27	Exploring Oxidation in the Remote Free Troposphere: Insights From Atmospheric Tomography (ATom). Journal of Geophysical Research D: Atmospheres, 2020, 125, e2019JD031685.	3.3	23
28	Global Atmospheric Budget of Acetone: Air‣ea Exchange and the Contribution to Hydroxyl Radicals. Journal of Geophysical Research D: Atmospheres, 2020, 125, e2020JD032553.	3.3	17
29	Siberian and temperate ecosystems shape Northern Hemisphere atmospheric CO ₂ seasonal amplification. Proceedings of the National Academy of Sciences of the United States of America, 2020, 117, 21079-21087.	7.1	27
30	Validation of Carbon Trace Gas Profile Retrievals from the NOAA-Unique Combined Atmospheric Processing System for the Cross-Track Infrared Sounder. Remote Sensing, 2020, 12, 3245.	4.0	23
31	Estimating US fossil fuel CO ₂ emissions from measurements of ¹⁴ C in atmospheric CO ₂ . Proceedings of the National Academy of Sciences of the United States of America, 2020, 117, 13300-13307.	7.1	65
32	Missing OH reactivity in the global marine boundary layer. Atmospheric Chemistry and Physics, 2020, 20, 4013-4029.	4.9	25
33	Investigating large methane enhancements in the U.S. San Juan Basin. Elementa, 2020, 8, .	3.2	8
34	Global-scale distribution of ozone in the remote troposphere from the ATom and HIPPO airborne field missions. Atmospheric Chemistry and Physics, 2020, 20, 10611-10635.	4.9	31
35	Investigating stratospheric changes between 2009 and 2018 with halogenated trace gas data from aircraft, AirCores, and a global model focusing on CFC-11. Atmospheric Chemistry and Physics, 2020, 20, 9771-9782.	4.9	10
36	Autonomous airborne mid-infrared spectrometer for high-precision measurements of ethane during the NASA ACT-America studies. Atmospheric Measurement Techniques, 2020, 13, 6095-6112.	3.1	2

#	Article	IF	CITATIONS
37	Data-driven Urban Methane Emission Estimates Based on Aircraft Observations: Sensing Considerations and Results. , 2020, , .		0
38	Urban Methane Emission Estimates Based on Aircraft and Satellite Observations. , 2020, , .		0
39	Sensitivity of Methane Emissions to Later Soil Freezing in Arctic Tundra Ecosystems. Journal of Geophysical Research G: Biogeosciences, 2019, 124, 2595-2609.	3.0	26
40	Large Fugitive Methane Emissions From Urban Centers Along the U.S. East Coast. Geophysical Research Letters, 2019, 46, 8500-8507.	4.0	83
41	An improved estimate for the <i>l^</i> ¹³ C and <i>l^</i> ¹⁸ O signatures of carbon monoxide produced from atmospheric oxidation of volatile organic compounds. Atmospheric	4.9	6
42	Chemiciny and Chysics, 20160, 69,0000700002 Ocean Biogeochemistry Control on the Marine Emissions of Brominated Very Shortâ€Lived Ozoneâ€Depleting Substances: A Machineâ€Learning Approach. Journal of Geophysical Research D: Atmospheres, 2019, 124, 12319-12339.	3.3	17
43	Methane emissions from oil and gas production on the North Slope of Alaska. Atmospheric Environment, 2019, 218, 116985.	4.1	8
44	Enhanced oceanic CO2 uptake along the rapidly changing West Antarctic Peninsula. Nature Climate Change, 2019, 9, 678-683.	18.8	62
45	The 2015–2016 carbon cycle as seen from OCO-2 and the global in situ network. Atmospheric Chemistry and Physics, 2019, 19, 9797-9831.	4.9	113
46	Intercomparison of atmospheric trace gas dispersion models: Barnett Shale case study. Atmospheric Chemistry and Physics, 2019, 19, 2561-2576.	4.9	24
47	Adaptation and performance assessment of a quantum and interband cascade laser spectrometer for simultaneous airborne in situ observation of CH ₄ , C ₂ 6, CO and N ₂ O.	3.1	29
48	Admospheric Weasurement Fechniques, 2019, 12, 12797-1285. Enhanced North American carbon uptake associated with El Niño. Science Advances, 2019, 5, eaaw0076.	10.3	45
49	The Observed Seasonal Cycle of Macronutrients in Drake Passage: Relationship to Fronts and Utility as a Model Metric. Journal of Geophysical Research: Oceans, 2019, 124, 4763-4783.	2.6	8
50	Mapping hydroxyl variability throughout the global remote troposphere via synthesis of airborne and satellite formaldehyde observations. Proceedings of the National Academy of Sciences of the United States of America, 2019, 116, 11171-11180.	7.1	58
51	Longâ€Term Measurements Show Little Evidence for Large Increases in Total U.S. Methane Emissions Over the Past Decade. Geophysical Research Letters, 2019, 46, 4991-4999.	4.0	35
52	Novel approaches to improve estimates of short-lived halocarbon emissions during summer from the Southern Ocean using airborne observations. Atmospheric Chemistry and Physics, 2019, 19, 14071-14090.	4.9	5
53	Evaluation of MOPITT VersionÂ7 joint TIR–NIR X _{CO} retrievals with TCCON. Atmospheric Measurement Techniques, 2019, 12, 5547-5572.	3.1	21
54	Summertime Atmospheric Boundary Layer Gradients of O 2 and CO 2 over the Southern Ocean. Journal of Geophysical Research D: Atmospheres, 2019, 124, 13439-13456.	3.3	2

#	Article	IF	CITATIONS
55	Synthesis of Urban CO ₂ Emission Estimates from Multiple Methods from the Indianapolis Flux Project (INFLUX). Environmental Science & Technology, 2019, 53, 287-295.	10.0	50
56	Topâ€Down CO Emissions Based On IASI Observations and Hemispheric Constraints on OH Levels. Geophysical Research Letters, 2018, 45, 1621-1629.	4.0	23
57	Source Partitioning of Methane Emissions and its Seasonality in the U.S. Midwest. Journal of Geophysical Research G: Biogeosciences, 2018, 123, 646-659.	3.0	18
58	Estimating regional-scale methane flux and budgets using CARVE aircraft measurements over Alaska. Atmospheric Chemistry and Physics, 2018, 18, 185-202.	4.9	15
59	The challenge of reconciling bottom-up agricultural methane emissions inventories with top-down measurements. Agricultural and Forest Meteorology, 2018, 248, 48-59.	4.8	25
60	The O2/N2 Ratio and CO2 Airborne Southern Ocean Study. Bulletin of the American Meteorological Society, 2018, 99, 381-402.	3.3	28
61	Three-dimensional methane distribution simulated with FLEXPART 8-CTM-1.1 constrained with observation data. Geoscientific Model Development, 2018, 11, 4469-4487.	3.6	10
62	CTDAS-Lagrange v1.0: a high-resolution data assimilation system for regional carbon dioxide observations. Geoscientific Model Development, 2018, 11, 3515-3536.	3.6	16
63	Bootstrap inversion technique for atmospheric trace gas source detection and quantification using long open-path laser measurements. Atmospheric Measurement Techniques, 2018, 11, 1565-1582.	3.1	12
64	Calibration and field testing of cavity ring-down laser spectrometers measuring CH ₄ , CO ₂ , and <i>1`</i> ¹³ CH _{4&a deployed on towers in the Marcellus Shale region. Atmospheric Measurement Techniques, 2018, 11, 1273-1295.}	amp;lt;/sul	b&⊉mp;gt;
65	Nitrous Oxide Emissions Estimated With the CarbonTrackerâ€Lagrange North American Regional Inversion Framework. Global Biogeochemical Cycles, 2018, 32, 463-485.	4.9	24
66	Anthropogenic and biogenic CO ₂ fluxes in the Boston urban region. Proceedings of the National Academy of Sciences of the United States of America, 2018, 115, 7491-7496.	7.1	110
67	Regional trace-gas source attribution using a field-deployed dual frequency comb spectrometer. Optica, 2018, 5, 320.	9.3	129
68	Accelerating rates of Arctic carbon cycling revealed by long-term atmospheric CO ₂ measurements. Science Advances, 2018, 4, eaao1167.	10.3	57
69	Utilizing the Drake Passage Time-series to understand variability and change in subpolar Southern Ocean <i>p</i> CO ₂ . Biogeosciences, 2018, 15, 3841-3855.	3.3	32
70	Assessment of methane emissions from the U.S. oil and gas supply chain. Science, 2018, 361, 186-188.	12.6	519
71	Biological and physical controls on O2/Ar, Ar and pCO2 variability at the Western Antarctic Peninsula and in the Drake Passage. Deep-Sea Research Part II: Topical Studies in Oceanography, 2017, 139, 77-88.	1.4	15
72	Methane, Black Carbon, and Ethane Emissions from Natural Gas Flares in the Bakken Shale, North Dakota. Environmental Science & Technology, 2017, 51, 5317-5325.	10.0	74

#	Article	IF	CITATIONS
73	Carbon dioxide sources from Alaska driven by increasing early winter respiration from Arctic tundra. Proceedings of the National Academy of Sciences of the United States of America, 2017, 114, 5361-5366.	7.1	149
74	Peak growing season gross uptake of carbon in North America is largest in the Midwest USA. Nature Climate Change, 2017, 7, 450-454.	18.8	39
75	Airborne Quantification of Methane Emissions over the Four Corners Region. Environmental Science & Technology, 2017, 51, 5832-5837.	10.0	52
76	U.S. CH ₄ emissions from oil and gas production: Have recent large increases been detected?. Journal of Geophysical Research D: Atmospheres, 2017, 122, 4070-4083.	3.3	47
77	Anthropogenic CO ₂ accumulation and uptake rates in the Pacific Ocean based on changes in the ¹³ C/ ¹² C of dissolved inorganic carbon. Global Biogeochemical Cycles, 2017, 31, 59-80.	4.9	18
78	Drivers and Environmental Responses to the Changing Annual Snow Cycle of Northern Alaska. Bulletin of the American Meteorological Society, 2017, 98, 2559-2577.	3.3	35
79	Considerable contribution of the Montreal Protocol to declining greenhouse gas emissions from the United States. Geophysical Research Letters, 2017, 44, 8075-8083.	4.0	30
80	Gradients of column CO ₂ across North America from the NOAA Global Greenhouse Gas Reference Network. Atmospheric Chemistry and Physics, 2017, 17, 15151-15165.	4.9	12
81	Quantifying methane emissions from natural gas production in north-eastern Pennsylvania. Atmospheric Chemistry and Physics, 2017, 17, 13941-13966.	4.9	54
82	Lower-tropospheric CO ₂ from near-infrared ACOS-GOSAT observations. Atmospheric Chemistry and Physics, 2017, 17, 5407-5438.	4.9	15
83	AirCore-HR: a high-resolution column sampling to enhance the vertical description of CH ₄ and CO ₂ . Atmospheric Measurement Techniques, 2017, 10, 2163-2181.	3.1	27
84	Tower measurement network of in-situ CO2, CH4, and CO in support of the Indianapolis FLUX (INFLUX) Experiment. Elementa, 2017, 5, .	3.2	31
85	Quantification of urban atmospheric boundary layer greenhouse gas dry mole fraction enhancements in the dormant season: Results from the Indianapolis Flux Experiment (INFLUX). Elementa, 2017, 5, .	3.2	24
86	Airborne DOAS retrievals of methane, carbon dioxide, and water vapor concentrations at high spatial resolution: application to AVIRIS-NG. Atmospheric Measurement Techniques, 2017, 10, 3833-3850.	3.1	72
87	A climate-scale satellite record for carbon monoxide: the MOPITT Version 7 product. Atmospheric Measurement Techniques, 2017, 10, 2533-2555.	3.1	69
88	Application of Gauss's theorem to quantify localized surface emissions from airborne measurements of wind and trace gases. Atmospheric Measurement Techniques, 2017, 10, 3345-3358.	3.1	86
89	Assessing the optimized precision of the aircraft mass balance method for measurement of urban greenhouse gas emission rates through averaging. Elementa, 2017, 5, .	3.2	46
90	Carbon monoxide isotopic measurements in Indianapolis constrain urban source isotopic signatures and support mobile fossil fuel emissions as the dominant wintertime CO source. Elementa, 2017, 5, .	3.2	13

#	Article	IF	CITATIONS
91	The Indianapolis Flux Experiment (INFLUX): A test-bed for developing urban greenhouse gas emission measurements. Elementa, 2017, 5, .	3.2	59
92	A multi-scale comparison of modeled and observed seasonal methane emissions in northern wetlands. Biogeosciences, 2016, 13, 5043-5056.	3.3	24
93	Bias corrections of GOSAT SWIR XCO ₂ and XCH ₄ with TCCON data and their evaluation using aircraft measurement data. Atmospheric Measurement Techniques, 2016, 9, 3491-3512.	3.1	40
94	Evaluation of wetland methane emissions across North America using atmospheric data and inverse modeling. Biogeosciences, 2016, 13, 1329-1339.	3.3	21
95	No significant increase in longâ€ŧerm CH ₄ emissions on North Slope of Alaska despite significant increase in air temperature. Geophysical Research Letters, 2016, 43, 6604-6611.	4.0	52
96	Lidar Characterization of Boundary Layer Transport and Mixing for Estimating Urban-Scale Greenhouse Gas Emissions. EPJ Web of Conferences, 2016, 119, 09001.	0.3	1
97	The influence of daily meteorology on boreal fire emissions and regional trace gas variability. Journal of Geophysical Research G: Biogeosciences, 2016, 121, 2793-2810.	3.0	9
98	Airborne methane remote measurements reveal heavy-tail flux distribution in Four Corners region. Proceedings of the National Academy of Sciences of the United States of America, 2016, 113, 9734-9739.	7.1	174
99	Highâ€resolution atmospheric inversion of urban CO ₂ emissions during the dormant season of the Indianapolis Flux Experiment (INFLUX). Journal of Geophysical Research D: Atmospheres, 2016, 121, 5213-5236.	3.3	219
100	A multiyear estimate of methane fluxes in Alaska from CARVE atmospheric observations. Global Biogeochemical Cycles, 2016, 30, 1441-1453.	4.9	36
101	Mesoscale modulation of airâ€sea <scp>CO</scp> ₂ flux in <scp>D</scp> rake <scp>P</scp> assage. Journal of Geophysical Research: Oceans, 2016, 121, 6635-6649.	2.6	23
102	Inverse modeling of pan-Arctic methane emissions at high spatial resolution: what can we learn from assimilating satellite retrievals and using different process-based wetland and lake biogeochemical models?. Atmospheric Chemistry and Physics, 2016, 16, 12649-12666.	4.9	27
103	Investigating Alaskan methane and carbon dioxide fluxes using measurements from the CARVE tower. Atmospheric Chemistry and Physics, 2016, 16, 5383-5398.	4.9	26
104	Quantifying atmospheric methane emissions from oil and natural gas production in the Bakken shale region of North Dakota. Journal of Geophysical Research D: Atmospheres, 2016, 121, 6101-6111.	3.3	99
105	Surrogate gas prediction model as a proxy for Δ ¹⁴ Câ€based measurements of fossil fuel CO ₂ . Journal of Geophysical Research D: Atmospheres, 2016, 121, 7489-7505.	3.3	1
106	Detecting regional patterns of changing CO ₂ flux in Alaska. Proceedings of the National Academy of Sciences of the United States of America, 2016, 113, 7733-7738.	7.1	33
107	Fugitive emissions from the Bakken shale illustrate role of shale production in global ethane shift. Geophysical Research Letters, 2016, 43, 4617-4623.	4.0	81
108	Continued emissions of carbon tetrachloride from the United States nearly two decades after its phaseout for dispersive uses. Proceedings of the National Academy of Sciences of the United States of America, 2016, 113, 2880-2885.	7.1	32

#	Article	IF	CITATIONS
109	Cold season emissions dominate the Arctic tundra methane budget. Proceedings of the National Academy of Sciences of the United States of America, 2016, 113, 40-45.	7.1	278
110	O3, CH4, CO2, CO, NO2 and NMHC aircraft measurements in the Uinta Basin oil and gas region under low and high ozone conditions in winter 2012 and 2013. Elementa, 2016, 4, .	3.2	8
111	A multi-decade record of high-quality <i>f</i> CO ₂ data in version 3 of the Surface Ocean CO ₂ Atlas (SOCAT). Earth System Science Data, 2016, 8, 383-413.	9.9	413
112	Toward quantification and source sector identification of fossil fuel CO ₂ emissions from an urban area: Results from the INFLUX experiment. Journal of Geophysical Research D: Atmospheres, 2015, 120, 292-312.	3.3	140
113	U.S. emissions of HFCâ€134a derived for 2008–2012 from an extensive flaskâ€air sampling network. Journal of Geophysical Research D: Atmospheres, 2015, 120, 801-825.	3.3	30
114	Atmospheric transport simulations in support of the Carbon in Arctic Reservoirs Vulnerability Experiment (CARVE). Atmospheric Chemistry and Physics, 2015, 15, 4093-4116.	4.9	22
115	Understanding high wintertime ozone pollution events in an oil- and natural gas-producing region of the western US. Atmospheric Chemistry and Physics, 2015, 15, 411-429.	4.9	154
116	Inverse modelling of CH ₄ emissions for 2010–2011 using different satellite retrieval products from GOSAT and SCIAMACHY. Atmospheric Chemistry and Physics, 2015, 15, 113-133.	4.9	126
117	Estimating global and North American methane emissions with high spatial resolution using GOSAT satellite data. Atmospheric Chemistry and Physics, 2015, 15, 7049-7069.	4.9	225
118	Recent evidence for a strengthening CO ₂ sink in the Southern Ocean from carbonate system measurements in the Drake Passage (2002–2015). Geophysical Research Letters, 2015, 42, 7623-7630.	4.0	70
119	Seasonal climatology of CO ₂ across North America from aircraft measurements in the NOAA/ESRL Global Greenhouse Gas Reference Network. Journal of Geophysical Research D: Atmospheres, 2015, 120, 5155-5190.	3.3	153
120	Reconciling divergent estimates of oil and gas methane emissions. Proceedings of the National Academy of Sciences of the United States of America, 2015, 112, 15597-15602.	7.1	209
121	Black Carbon Emissions from the Bakken Oil and Gas Development Region. Environmental Science and Technology Letters, 2015, 2, 281-285.	8.7	49
122	Aircraft-Based Estimate of Total Methane Emissions from the Barnett Shale Region. Environmental Science & Technology, 2015, 49, 8124-8131.	10.0	190
123	Airborne Ethane Observations in the Barnett Shale: Quantification of Ethane Flux and Attribution of Methane Emissions. Environmental Science & Technology, 2015, 49, 8158-8166.	10.0	100
124	Aircraft-Based Measurements of Point Source Methane Emissions in the Barnett Shale Basin. Environmental Science & Technology, 2015, 49, 7904-7913.	10.0	93
125	Estimates of net community production in the Southern Ocean determined from time series observations (2002–2011) of nutrients, dissolved inorganic carbon, and surface ocean pCO2 in Drake Passage. Deep-Sea Research Part II: Topical Studies in Oceanography, 2015, 114, 49-63.	1.4	43
126	The reinvigoration of the Southern Ocean carbon sink. Science, 2015, 349, 1221-1224.	12.6	331

#	Article	IF	CITATIONS
127	Quantification and source apportionment of the methane emission flux from the city of Indianapolis. Elementa, 2015, 3, .	3.2	50
128	Evaluation of the airborne quantum cascade laser spectrometer (QCLS) measurements of the carbon and greenhouse gas suite – CO ₂ , CH ₄ , N ₂ O, and CO – during the CalNex and HIPPO campaigns. Atmospheric Measurement Techniques, 2014, 7, 1509-1526.	3.1	75
129	Validation of XCH ₄ derived from SWIR spectra of GOSAT TANSO-FTS with aircraft measurement data. Atmospheric Measurement Techniques, 2014, 7, 2987-3005.	3.1	32
130	The MOPITT Version 6 product: algorithm enhancements and validation. Atmospheric Measurement Techniques, 2014, 7, 3623-3632.	3.1	92
131	Measurements of hydrogen sulfide (H ₂ S) using PTR-MS: calibration, humidity dependence, inter-comparison and results from field studies in an oil and gas production region. Atmospheric Measurement Techniques, 2014, 7, 3597-3610.	3.1	26
132	A Cost-Effective Trace Gas Measurement Program for Long-Term Monitoring of the Stratospheric Circulation. Bulletin of the American Meteorological Society, 2014, 95, 147-155.	3.3	11
133	Drake Passage Oceanic pCO2: Evaluating CMIP5 Coupled Carbon–Climate Models Using in situ Observations. Journal of Climate, 2014, 27, 76-100.	3.2	18
134	A Low-Cost System for Measuring Horizontal Winds from Single-Engine Aircraft. Journal of Atmospheric and Oceanic Technology, 2014, 31, 1312-1320.	1.3	37
135	Frequency-comb-based remote sensing of greenhouse gases over kilometer air paths. Optica, 2014, 1, 290.	9.3	296
136	Methane emissions from Alaska in 2012 from CARVE airborne observations. Proceedings of the National Academy of Sciences of the United States of America, 2014, 111, 16694-16699.	7.1	58
137	Toward a better understanding and quantification of methane emissions from shale gas development. Proceedings of the National Academy of Sciences of the United States of America, 2014, 111, 6237-6242.	7.1	296
138	High winter ozone pollution from carbonyl photolysis in an oil and gas basin. Nature, 2014, 514, 351-354.	27.8	265
139	Climatological distributions of pH, pCO2, total CO2, alkalinity, and CaCO3 saturation in the global surface ocean, and temporal changes at selected locations. Marine Chemistry, 2014, 164, 95-125.	2.3	354
140	Demonstration of an Ethane Spectrometer for Methane Source Identification. Environmental Science & Technology, 2014, 48, 8028-8034.	10.0	101
141	Improving stratospheric transport trend analysis based on SF ₆ and CO ₂ measurements. Journal of Geophysical Research D: Atmospheres, 2014, 119, 14,110.	3.3	57
142	Assessment of uncertainties of an aircraft-based mass balance approach for quantifying urban greenhouse gas emissions. Atmospheric Chemistry and Physics, 2014, 14, 9029-9050.	4.9	109
143	TransCom N ₂ O model inter-comparison – Part 1: Assessing the influence of transport and surface fluxes on tropospheric N ₂ O variability. Atmospheric Chemistry and Physics, 2014, 14, 4349-4368.	4.9	34
144	CarbonTracker-CH ₄ : an assimilation system for estimating emissions of atmospheric methane. Atmospheric Chemistry and Physics, 2014, 14, 8269-8293.	4.9	187

#	Article	IF	CITATIONS
145	A new look at methane and nonmethane hydrocarbon emissions from oil and natural gas operations in the Colorado Denverâ€Julesburg Basin. Journal of Geophysical Research D: Atmospheres, 2014, 119, 6836-6852.	3.3	257
146	An update to the Surface Ocean CO ₂ Atlas (SOCAT version 2). Earth System Science Data, 2014, 6, 69-90.	9.9	158
147	Methane emissions estimate from airborne measurements over a western United States natural gas field. Geophysical Research Letters, 2013, 40, 4393-4397.	4.0	414
148	Enhanced Seasonal Exchange of CO ₂ by Northern Ecosystems Since 1960. Science, 2013, 341, 1085-1089.	12.6	329
149	Constraints on emissions of carbon monoxide, methane, and a suite of hydrocarbons in the Colorado Front Range using observations of ¹⁴ CO ₂ . Atmospheric Chemistry and Physics. 2013. 13. 11101-11120.	4.9	27
150	High accuracy measurements of dry mole fractions of carbon dioxide and methane in humid air. Atmospheric Measurement Techniques, 2013, 6, 837-860.	3.1	151
151	Long-term greenhouse gas measurements from aircraft. Atmospheric Measurement Techniques, 2013, 6, 511-526.	3.1	87
152	A multi-year record of airborne CO ₂ observations in the US Southern Great Plains. Atmospheric Measurement Techniques, 2013, 6, 751-763.	3.1	44
153	Atmospheric Carbon Dioxide Variability in the Community Earth System Model: Evaluation and Transient Dynamics during the Twentieth and Twenty-First Centuries. Journal of Climate, 2013, 26, 4447-4475.	3.2	48
154	Anthropogenic emissions of methane in the United States. Proceedings of the National Academy of Sciences of the United States of America, 2013, 110, 20018-20022.	7.1	437
155	Background error covariance estimation for atmospheric CO 2 data assimilation. Journal of Geophysical Research D: Atmospheres, 2013, 118, 10,140.	3.3	22
156	Atmospheric CH ₄ in the first decade of the 21st century: Inverse modeling analysis using SCIAMACHY satellite retrievals and NOAA surface measurements. Journal of Geophysical Research D: Atmospheres, 2013, 118, 7350-7369.	3.3	226
157	Allocation of Terrestrial Carbon Sources Using ¹⁴ CO ₂ : Methods, Measurement, and Modeling. Radiocarbon, 2013, 55, 1484-1495.	1.8	35
158	Atmospheric column-averaged mole fractions of carbon dioxide at 53 aircraft measurement sites. Atmospheric Chemistry and Physics, 2013, 13, 5265-5275.	4.9	20
159	Corrigendum to "Atmospheric column-averaged mole fractions of carbon dioxide at 53 aircraft measurement sites" published in Atmos. Chem. Phys. 13, 5265–5275, 2013. Atmospheric Chemistry and Physics, 2013, 13, 9213-9216.	4.9	2
160	Validation of XCO ₂ derived from SWIR spectra of GOSAT TANSO-FTS with aircraft measurement data. Atmospheric Chemistry and Physics, 2013, 13, 9771-9788.	4.9	106
161	Tropospheric SF ₆ : Age of air from the Northern Hemisphere midlatitude surface. Journal of Geophysical Research D: Atmospheres, 2013, 118, 11,429.	3.3	37
162	Detection of methane depletion associated with stratospheric intrusion by atmospheric infrared sounder (AIRS). Geophysical Research Letters, 2013, 40, 2455-2459.	4.0	21

#	Article	IF	CITATIONS
163	TransCom model simulations of methane: Comparison of vertical profiles with aircraft measurements. Journal of Geophysical Research D: Atmospheres, 2013, 118, 3891-3904.	3.3	24
164	Sea–air CO ₂ fluxes in the Southern Ocean for the period 1990–2009. Biogeosciences, 2013, 10, 4037-4054.	3.3	162
165	Global ocean carbon uptake: magnitude, variability and trends. Biogeosciences, 2013, 10, 1983-2000.	3.3	276
166	Accurate measurements of carbon monoxide in humid air using the cavity ring-down spectroscopy (CRDS) technique. Atmospheric Measurement Techniques, 2013, 6, 1031-1040.	3.1	64
167	An integrated flask sample collection system for greenhouse gas measurements. Atmospheric Measurement Techniques, 2012, 5, 2321-2327.	3.1	33
168	Assessing filtering of mountaintop CO ₂ mole fractions for application to inverse models of biosphere-atmosphere carbon exchange. Atmospheric Chemistry and Physics, 2012, 12, 2099-2115.	4.9	20
169	Constraining the CO ₂ budget of the corn belt: exploring uncertainties from the assumptions in a mesoscale inverse system. Atmospheric Chemistry and Physics, 2012, 12, 337-354.	4.9	145
170	Hydrocarbon emissions characterization in the Colorado Front Range: A pilot study. Journal of Geophysical Research, 2012, 117, .	3.3	359
171	The observed evolution of oceanic pCO ₂ and its drivers over the last two decades. Global Biogeochemical Cycles, 2012, 26, .	4.9	83
172	Linking emissions of fossil fuel CO ₂ and other anthropogenic trace gases using atmospheric ¹⁴ CO ₂ . Journal of Geophysical Research, 2012, 117, .	3.3	121
173	Seasonal variations in N ₂ O emissions from central California. Geophysical Research Letters, 2012, 39, .	4.0	30
174	Longâ€ŧerm ozone trends at rural ozone monitoring sites across the United States, 1990–2010. Journal of Geophysical Research, 2012, 117, .	3.3	180
175	North American CO ₂ exchange: inter-comparison of modeled estimates with results from a fine-scale atmospheric inversion. Biogeosciences, 2012, 9, 457-475.	3.3	102
176	The Changing Carbon Cycle in the Southern Ocean. Oceanography, 2012, 25, 26-37.	1.0	104
177	High-Resolution Underway Upper Ocean and Surface Atmospheric Observations in Drake Passage: Synergistic Measurements for Climate Science. Oceanography, 2012, 25, 70-81.	1.0	19
178	Atmospheric CO ₂ inversion validation using vertical profile measurements: Analysis of four independent inversion models. Journal of Geophysical Research, 2011, 116, .	3.3	41
179	Tropospheric distribution and variability of N ₂ O: Evidence for strong tropical emissions. Geophysical Research Letters, 2011, 38, .	4.0	78
180	Assessment of fossil fuel carbon dioxide and other anthropogenic trace gas emissions from airborne measurements over Sacramento, California in spring 2009. Atmospheric Chemistry and Physics, 2011, 11, 705-721.	4.9	148

#	Article	IF	CITATIONS
181	Short Note: Natural seasonal variability of aragonite saturation state within two Antarctic coastal ocean sites. Antarctic Science, 2011, 23, 411-412.	0.9	28
182	The seasonal cycle amplitude of total column CO2: Factors behind the model-observation mismatch. Journal of Geophysical Research, 2011, 116, n/a-n/a.	3.3	24
183	AirCore: An Innovative Atmospheric Sampling System. Journal of Atmospheric and Oceanic Technology, 2010, 27, 1839-1853.	1.3	145
184	Atmospheric constraints on 2004 emissions of methane and nitrous oxide in North America from atmospheric measurements and a receptor-oriented modeling framework. Journal of Integrative Environmental Sciences, 2010, 7, 125-133.	2.5	20
185	Carbon monoxide mixing ratios over Oklahoma between 2002 and 2009 retrieved from Atmospheric Emitted Radiance Interferometer spectra. Atmospheric Measurement Techniques, 2010, 3, 1319-1331.	3.1	19
186	Calibration of the Total Carbon Column Observing Network using aircraft profile data. Atmospheric Measurement Techniques, 2010, 3, 1351-1362.	3.1	441
187	Seasonal forcing of summer dissolved inorganic carbon and chlorophyll <i>a</i> on the western shelf of the Antarctic Peninsula. Journal of Geophysical Research, 2010, 115, .	3.3	23
188	Midâ€upper tropospheric methane in the high Northern Hemisphere: Spaceborne observations by AIRS, aircraft measurements, and model simulations. Journal of Geophysical Research, 2010, 115, .	3.3	44
189	A multiâ€decadal delay in the onset of corrosive â€~acidified' waters in the Ross Sea of Antarctica due to strong airâ€sea CO ₂ disequilibrium. Geophysical Research Letters, 2010, 37, .	4.0	48
190	Regional US carbon sinks from three-dimensional atmospheric CO ₂ sampling. Proceedings of the United States of America, 2010, 107, 18348-18353.	7.1	61
191	Demonstration of highâ€precision continuous measurements of water vapor isotopologues in laboratory and remote field deployments using wavelengthâ€scanned cavity ringâ€down spectroscopy (WSâ€CRDS) technology. Rapid Communications in Mass Spectrometry, 2009, 23, 2534-2542.	1.5	273
192	Aircraft-Based Measurements of the Carbon Footprint of Indianapolis. Environmental Science & Technology, 2009, 43, 7816-7823.	10.0	167
193	Climatological mean and decadal change in surface ocean pCO2, and net sea–air CO2 flux over the global oceans. Deep-Sea Research Part II: Topical Studies in Oceanography, 2009, 56, 554-577.	1.4	1,540
194	Regional surface flux of CO2 inferred from changes in the advected CO2 column density. Agricultural and Forest Meteorology, 2009, 149, 1674-1685.	4.8	16
195	Advances in Quantifying Air-Sea Gas Exchange and Environmental Forcing. Annual Review of Marine Science, 2009, 1, 213-244.	11.6	552
196	CO ₂ retrievals from the Atmospheric Infrared Sounder: Methodology and validation. Journal of Geophysical Research, 2008, 113, .	3.3	75
197	Characterization and validation of methane products from the Atmospheric Infrared Sounder (AIRS). Journal of Geophysical Research, 2008, 113, .	3.3	137
198	Photosynthetic Control of Atmospheric Carbonyl Sulfide During the Growing Season. Science, 2008, 322, 1085-1088.	12.6	196

#	Article	IF	CITATIONS
199	Weak Northern and Strong Tropical Land Carbon Uptake from Vertical Profiles of Atmospheric CO2. Science, 2007, 316, 1732-1735.	12.6	775
200	An atmospheric perspective on North American carbon dioxide exchange: CarbonTracker. Proceedings of the United States of America, 2007, 104, 18925-18930.	7.1	895
201	Constraining global air-sea gas exchange for CO2with recent bomb14C measurements. Global Biogeochemical Cycles, 2007, 21, n/a-n/a.	4.9	442
202	On the global distribution, seasonality, and budget of atmospheric carbonyl sulfide (COS) and some similarities to CO2. Journal of Geophysical Research, 2007, 112, .	3.3	213
203	New constraints on Northern Hemisphere growing season net flux. Geophysical Research Letters, 2007, 34, .	4.0	147
204	A direct carbon budgeting approach to infer carbon sources and sinks. Design and synthetic application to complement the NACP observation network. Tellus, Series B: Chemical and Physical Meteorology, 2006, 58, 366-375.	1.6	17
205	Impacts of Shortwave Penetration Depth on Large-Scale Ocean Circulation and Heat Transport. Journal of Physical Oceanography, 2005, 35, 1103-1119.	1.7	154
206	The annual cycle of surface water CO2 And O2 in the Ross Sea: A model for gas exchange on the continental shelves of Antarctica. Antarctic Research Series, 2003, , 295-312.	0.2	57
207	Global sea–air CO2 flux based on climatological surface ocean pCO2, and seasonal biological and temperature effects. Deep-Sea Research Part II: Topical Studies in Oceanography, 2002, 49, 1601-1622.	1.4	1,506
208	Seasonal evolution of hydrographic properties in the Ross Sea, Antarctica, 1996–1997. Deep-Sea Research Part II: Topical Studies in Oceanography, 2000, 47, 3095-3117.	1.4	84
209	Biogeochemical regimes, net community production and carbon export in the Ross Sea, Antarctica. Deep-Sea Research Part II: Topical Studies in Oceanography, 2000, 47, 3369-3394.	1.4	139
210	Nutrient and carbon removal ratios and fluxes in the Ross Sea, Antarctica. Deep-Sea Research Part II: Topical Studies in Oceanography, 2000, 47, 3395-3421.	1.4	109
211	Effect of calcium carbonate saturation state on the calcification rate of an experimental coral reef. Global Biogeochemical Cycles, 2000, 14, 639-654.	4.9	496